

# **A multiobjective gradient based dose optimization algorithm for external beam conformal radiotherapy**

*C. Cotrutz<sup>\*(1)</sup>, M. Lahanas<sup>\*\*\*(2)</sup>, C. Kappas<sup>\*(3)</sup> and D. Baltas<sup>\*\*\*(4)</sup>*

\* Department of Medical Physics, University of Patras, School of Medicine, GR-26500 Rio, Patras, Greece.

\*\* Department of Medical Physics & Engineering, Strahlenklinik Klinikum Offenbach, 63069 Offenbach, Germany

Short Title: A multiobjective gradient based dose optimization algorithm

<sup>(1)</sup> and “Alex. I. Cuza” University, Dept. of Medical Physics, Blvd. Carol 11, RO-6600 Iasi, Romania  
e-mail: cotrutz@med.upatras.gr

<sup>(2)</sup> e-mail: mlahanas@gmx.de

<sup>(3)</sup> e-mail: kappas@med.upatras.gr

<sup>(4)</sup> and Institute of Communication & Computer Systems, National Technical University of Athens, 15773 Zografou, Athens, Greece; e-mail: dbaltas@compuserve.com

## **Abstract**

A multiobjective gradient based algorithm has been developed for the purpose of dose distribution optimization in external beam conformal radiotherapy. This algorithm is based on the concept to gather the values of all objectives in a single value. The weighting factors of the composite objective values are varied in different steps, allowing the reconstruction of the trade-off surfaces (three or more objectives) or curves (two objectives), which define the boundary between the feasible and non-feasible domain regions. The analysis of these curves allows the decision-maker to select the solution that best fits the clinical goals. In contrast to all the other algorithms, our method provides not a single solution but a sample of solutions representing all possible clinical importance factors (weights) for the used objectives. The application of this algorithm for two test cases shows that a correct selection of the importance factors to multiply the individual objectives in the global objective value is not trivial and that the location and shape of the boundary region between the feasible and non-feasible solution regions are case dependent. Provided that the individual objective functions are analytically differentiable and that the number of objectives is the range of 2-3, the computation times are acceptable for clinical use. Furthermore, the optimization for a unique combination of importance factors within the aggregate objective function is performed in less than one minute.

Key words: conjugate gradient algorithm, multiobjective optimization, conformal radiotherapy, IMRT

## 1.- Introduction

The conformal radiotherapy term defines those radiation therapy techniques, which aim at delivering as high as possible a uniform dose to the planning target volume (PTV), while concomitantly sparing as much as possible normal tissues and the organs at risk (OARs). These goals are currently achieved by using the computerized inverse planning systems that are capable to determine the optimal beam intensity profiles which would deliver to the patient that dose which is the closest to the prescribed one. The core of an inverse planning system is represented by the optimization engine, which handles the trade-off between different treatment objectives and accordingly adjusts in an iterative fashion the values of the beamlet intensities.

Two major approaches exist to date for the optimization algorithms: deterministic and stochastic. Both approaches quantify the goals achievement using objective functions that express either biologic responses to radiation (Mohan *et al.* 1992, Wang *et al.* 1995, Söderstrom and Brahme 1993, Gustafsson *et al.* 1994) or measures of how far is the physical dose distribution from the desired and prescribed one (Webb 1989, Mageras and Mohan 1993, Bortfeld *et al.* 1990).

Two factors affecting the optimization performance and its outcome are the form of the objective function and the optimization strategy. Most of the objective functions considered to be minimized or maximized in the dose-based optimization methods are in form of weighted sums of variances (Bortfeld *et al.* 1990), each term accounting for how well one of the treatment goal is achieved. By differently weighting the objectives within the aggregate form of the objective function, the optimization algorithm acts with more pressure towards achieving the treatment goal with the largest weight. The overall performance of the optimization is therefore linked to the knowledge of the individual weighting (or importance) factors, because the multiobjective problem is reduced to a single objective case prior to optimization. The usual treatments normally incorporate many objectives, which most of the time are competing one against the other. Therefore to date, the inverse planning process is still a trial and error one due to the multiple possible combinations of individual weighting factors of the objectives. The determination of these weighting factors is not trivial and most of publications report an empirical estimated single set of them. Furthermore, their appropriate values differ from clinical case to clinical case. This implies that for any new clinical case a lot of effort is necessary for their determination.

The problem of proper importance factor selection in external radiotherapy has been addressed by several authors. Xing *et al.* (1999) have proposed a method of optimizing the importance factors of a quadratic objective function. The process evolves in two stages. Firstly, the beamlet weights are optimized by minimizing the quadratic objective function seeded with an initial set of importance factors. In the second stage, based on a DVH score function calculated from the dose distribution obtained with the current estimate of the beamlet weights, the importance factors values are optimized using a multidimensional gradient based method. The iterations stop when the change of the DVH score function is less than a pre-chosen precision. Following the same pattern of two-step-optimization, Wu and Zhu (2000) propose a genetic algorithm that determines both the importance factors and the weights of the open beams to be used in the treatment. Both methods can be included within the frame of generically named multiobjective decision theory, as proposed for radiation therapy by Yu (1997).

Our approach is based on the following concept: (a) An optimization engine is utilized that provides a representative set of all possible solutions and (b) Decision process where user (radiation oncologist) selects from this set the most appropriate one with the help of a DVH-based analysis of the dose distributions.

The optimization algorithm described in this paper is gradient based and exploits the richness of all feasible solutions for a given set of clinical prescriptions offering thus to the decision-maker the possibility to chose from different alternatives. The decision process is based on the study of the trade-off curves or surfaces representing individual objectives. The objectives trade-off curves are determined by feeding an optimization engine with different possible combinations of importance factors. Therefore, our approach is a multiobjective based optimization. Known under the name of Pareto frontiers, these trade-off curves are built up from optimal points characterized by the fact that no improvement in one objective can occur without degradation in at least one of the remaining objectives. The optimization algorithm is a conjugate-gradient one and uses as variables to be optimized the square roots of the beamlet weights. Therefore, one of its strength is that it avoids *non-physical* solutions with negative weights. This simple mapping technique accelerates the optimization process by avoiding the use of additional constraints.

The present work is organized in four main sections. The next section of this paper gives an insight into the multiobjective optimization theory and describes the used optimization algorithm and strategy. The third section uses two test cases to demonstrate the achievable results of the current approach while the last section points out the potential and limitations of the developed gradient based multiobjective optimization.

## 2.- Method and materials

The dose optimization algorithm presented is a stand-alone module. It communicates for the input-output data with a home-made Treatment Planning System (TPS) earlier described by Cotrutz *et al.* (1998). The typical optimization follows two steps. In a first instance, according to the patient geometry and planner's beam set-up the home-made TPS produces a set of data files containing matrix indices of different structures, dose deposition coefficients, and the prescription matrix for all the structures involved in the optimization. These files are read and then used by the independent optimization module to perform the beamlet weights optimization according the specified criteria. The optimization results are fed back to the home-made TPS where the quality of plans is assessed using DVHs and dose distributions.

### 2.1.- Multiobjective optimization

The multiobjective optimization (called also multi-criteria or vector optimization) can be defined as the problem of determining (Deb 1999) a vector of decision variables which satisfies constraints and optimizes a vector function whose elements represent the objective functions. These functions form a mathematical description of the performance criteria, which are usually in conflict one with each other. Hence, the term optimize means finding such a solution which would give the values of all objective functions acceptable to the designer.

If one would like to describe mathematically the multiobjective optimization for the IMRT problem then this can be reduced to finding the sets  $\mathbf{x}(x_1, x_2, \dots, x_n)$  of beamlet weights, where  $x_1, x_2, \dots, x_n \geq 0$ . Every element of the set which represent one possible solution of the problem should satisfy a set of inequality constraints  $g_i(\mathbf{x}) \geq 0$ , where  $i = 1, 2, \dots, m$ . Note that these constraints apply on the doses calculated at different locations of the dose matrix. Any possible solution  $\mathbf{x}$  is mapped into the objective space  $\mathbf{F}$  by a vector of  $k$  objective functions  $\mathbf{f}(f_1(\mathbf{x}), \dots, f_k(\mathbf{x}))$ . Here  $k$  denotes the number of objectives. For the IMRT case, the vector of objective functions could be represented by objective functions defining the PTV dose homogeneity and the set of penalty functions for every critical structure. The optimization process is then reduced to finding  $\mathbf{x}$  by minimizing (or maximizing) the value in  $\mathbf{F}$  obtained by applying the  $\mathbf{f}(f_1(\mathbf{x}), \dots, f_k(\mathbf{x}))$  operator to the decision variable  $\mathbf{x}$ . The solutions mapped into the  $\mathbf{F}$  set can be ranked according their performances against each objective. If one considers a two-objective minimization (*Figure 1*), the solutions characterized by the  $\mathbf{F}$  values located at the interface  $\mathbf{AB}$  represent the best possible ones. To exemplify, we compare solutions 1, 2 and 3 with the solution numbered with 4. The first three solutions are better than 4 with respect to at least one objective. This means that solutions 1, 2 and 3 dominate solution 4. If we compare just the solutions 1, 2 and 3, we can see that they are somehow equivalent, in the sense that no improvement of an objective value can occur without the degradation of the remaining objective value. The solutions corresponding to the  $\mathbf{F}$  values on the  $\mathbf{AB}$  interface are called *Pareto* solutions and form the *Pareto frontier* or *set*. Mathematically, a solution  $\mathbf{x}^*$  that belongs to the  $\mathbf{X}$  domain is Pareto optimal if there does not exist any other solution  $\mathbf{x}$  in  $\mathbf{X}$  such that  $f_i(\mathbf{x}) \leq f_i(\mathbf{x}^*)$  for all  $i = 1, \dots, k$  objectives and  $f_j(\mathbf{x}) < f_j(\mathbf{x}^*)$  for at least one  $j \in \{1, \dots, k\}$  They are characterized by the fact that no improvement in one objective value can occur without

deterioration of at least one of the other objective values. Thus, the *Pareto* solutions describe the objectives trade-off. They lie at the boundary between the feasible and infeasible objective domains. The goal of the minimization is then to determine those solutions corresponding to the *Pareto frontier*.

## 2.2. Optimization strategy

If the *Pareto* set is determined, then the decision-maker can select the most appropriate solution that would better suit the clinical prescriptions. It is hence important to provide the decision-maker a quasi-complete set of solution, because the initial prescription may not be physically achievable. He should then do the compromise and select the solution with the least risk.

The current multiobjective optimization approach combines the individual objective values (*e.g.* target homogeneity, dose variance for different critical structures against their critical dose values) into an aggregate function. For  $k$  objectives, the aggregate function (or cost function) is expressed as:

$$w_1 \cdot f_1(x) + w_2 \cdot f_2(x) + \dots + w_k \cdot f_k(x) \quad (1)$$

where  $w_1, \dots, w_k$  are the weights or the importance factors expressing the importance of each objective term in the optimization process, and  $w_1 + w_2 + \dots + w_k = 1$ . The way the current optimization method obtains the points on the *Pareto* frontier is the use of several combinations of importance factors. The generation of points by minimizing weighted sums of objectives is limited to convex sets and therefore imposes some limitations on the constraints to be used in the optimization process, in order to ensure convergence to a unique minimum. Therefore, according to Deasy (1997), the current optimization strategy does not consider dose-volume constraints, which severely restricts the feasible region into possible non convex sets.

## 2.3.- Objective function

The objective functions used in our study are of a dose-based type and mathematically express the treatment goals related to the Planning Target Volume (PTV) and Organs At Risk (OARs) as follows:

$$f_{PTV} = \frac{1}{n_{PTV}} \cdot \sum_{i=1}^{n_{PTV}} \frac{(D_i - \bar{D}_{PTV})^2}{\bar{D}_{PTV}^2} \quad (2)$$

$$f_{OAR_j} = \frac{1}{n_{OAR_j}} \cdot \sum_{i=1}^{n_{OAR_j}} \frac{\mathbf{d}_i \cdot (D_i - D_{OAR_j}^{crit})^2}{D_{OAR_j}^{crit}{}^2} \quad (3)$$

$$\mathbf{d}_i = \begin{cases} 0 & \text{if } D_i \leq D_{OAR_j}^{crit} \\ 1 & \text{if } D_i > D_{OAR_j}^{crit} \end{cases} \quad (4)$$

where  $D_i$  is the current iteration calculated dose,  $\bar{D}_{PTV}$  is the current iteration mean PTV dose,  $D_{OAR_j}^{crit}$  is the critical dose value for the  $j$ -th OAR,  $n_{OAR_j}$  is the number of points of the  $j$ -th OAR for which the  $D_i \leq D_{OAR_j}^{crit}$  condition is not met and  $n_{PTV}$  represents the total number of the PTV dose calculation points. In relations (3) and (4),  $\mathbf{d}_i$  represents the

step function that “decides” which dose points are to be penalized and to contribute to the value of the objective function for that specific OAR. In other words, the target objective regards the dose homogeneity within the PTV and is expressed in term of dose variance against the mean dose. The objective functions for the critical structures are of the same form as for the PTV, but involve the dose variances against critical dose values specific only for those particular OARs.

The global objective function to be minimized according to the optimization strategy described in the previous section is therefore:

$$f = w_{PTV} \cdot f_{PTV} + \sum_{j=1}^{N_{OAR}} w_{OAR_j} \cdot f_{OAR_j} \quad (5) \quad \text{and}$$

$$w_{PTV} + \sum_{j=1}^{N_{OAR}} w_{OAR_j} = 1 \quad (6)$$

In equations (5) and (6),  $w_{PTV}$  and  $w_{OAR_j}$  are the importance factors of the target’s objective and of the  $j$ -th organ at risk, while  $N_{OAR}$  represents the number of the critical structures. This formulation of the objective function aims at expressing better the goal of obtaining trade-off curves PTV–OAR<sub>j</sub> when different importance factors are assigned to the PTV and OARs.

## 2.4.- Conjugate gradient algorithm

In our study a Polak-Ribiere variant of the Fletcher-Reeves conjugate gradient optimization algorithm (Press *et al.* 1992) is used. The multidimensional optimization process is carried out iteratively, in two major steps. Firstly, the direction of optimization is chosen and secondly, along the chosen direction, a line minimization is performed. The algorithm itself does not limit the solution to be non-negative. Most of the IMRT gradient-based dose optimization algorithms known to date (Hristov and Fallone 1997 1998, Spirou and Chui 1997, Wu and Mohan 2000) either impose positivity constraints to the solution (in order to ensure their physical meaning), or truncate to zero every iteration those solution negative components. The effect of these techniques is either to increase the number of parameters by a factor of two in the case of the constrained optimization or to reduce the quality of the optimization process for the case of truncation. In order to avoid these inconveniences in our algorithm, we implemented a mapping scheme that transforms the decision variables (beamlet weights) from  $x_k$  into  $x'_k = x_k^{1/2}$ . This means that the search of the minimization directions and of the minimum along a line occurs normally within the whole space of beamlet square roots. The difference with the other implementations is consistent with the squaring operator, which is applied to the beamlet weights when switching from the variables space to the objectives space. This operator ensures the positivity of the solutions and in fact, transforms every line of search into its positive part. It is worth mentioning that at the end of the optimization cycle for one Pareto point, the negative square roots of the beamlet weights have very small, almost zero values. Therefore, the overall effect of the mirroring process is similar to constraining the variables space, but without imposing explicit conditions.

The algorithm whose flow chart is depicted in *Figure 2* starts with an initialization of beamlet weights square roots. Following, the current iteration dose values are calculated using the dose deposition matrix coefficients and the initial values of the beamlet weights. Accordingly, the objective values are calculated according to equations (2) and

(3) and then the first derivative of the aggregate objective function with respect to each of the variables is computed. This latter step allows the determination of the appropriate direction the line minimization has to follow. Once the minimum along a direction is found one iteration is completed and the process continues until a predetermined number of iterations is reached, or a tolerance condition on the aggregate objective function is met. At this point, the solution for the given set of importance factors is obtained and following, their values are re-actualized according to a predetermined schema. Generally, several objectives can be implemented in the algorithm described above, meaning that loops inside the main loop depicted in the figure's 2 flow diagram could account for different importance factor values of the newly added OARs. The process continues until all the possible combinations for the importance factors steps are exhausted and all the needed Pareto solutions are generated.

### 3.- Results and Discussion

Two test cases were used for the assessment of the newly proposed algorithm. Case A is a simulated concave target with an organ at risk in an elliptical phantom. Case B is a prostate tumor with organs at risk being bladder, rectum, and the two femoral heads. The test case A was also used to assess the convergence rate of the gradient-based algorithm and to establish the value of the iterations number necessary to accomplish the objective minimization. These values were then used for test case B.

In our implementation a radiological pathlength dose computation model was used. The dose value to any calculation point is obtained by interpolating Tissue Maximum Ratios (TMR) and Off-Center Ratios (OCR) tables, derived from percentage depth dose and beam profiles measurements performed in a water phantom. The incident photon fluence variation across the transversal section of the beam was taken into account by dividing the beam into pencils and assigning different transmission factors for each pencil. This value is then multiplied to the dose obtained by interpolation in order to obtain the dose value for that specific calculation point located within the “shadow” of the pencil. The width of the pencil projected at the isocentre was 0.5 cm.

#### 3.1. C-shaped tumor

The simulated C-shaped tumor case consists of three structures, namely the PTV, the circular OAR located in the concavity of the PTV and the normal tissue (NT) considered as that volume (surface) that excludes the PTV and the OAR (*Figure 5*). Seven beams ( $14.0 \times 10.0 \text{ cm}^2$ ) were set at the following angles:  $5^\circ$ ,  $55^\circ$ ,  $105^\circ$ ,  $165^\circ$ ,  $215^\circ$ ,  $265^\circ$  and  $315^\circ$  degrees (respecting the IEC convention), respectively. This beam setup was used to assess the convergence rate of the optimization algorithm, and to establish thus the necessary number of iterations needed to achieve the best ratio of the aggregate objective value reduction. Two objectives were taken in consideration for the convergence assessment, namely the C-shaped Tumor (PTV) and the critical structure (OAR). *Figure 3* shows the dependence of the global objective value vs. the iteration number for three different combinations of the individual objectives. Each of the combinations was characterized by different values assigned to the importance factors, as described in the equation (5). For each of the three combinations, one can see that approximately 75 iterations are more than enough for the Polak-Ribiere variant of the Fletcher-Reeves conjugate gradient algorithm to reach the minimum plateau region. The global objective value after 75 iterations is reduced insignificantly.

For the C-shaped tumor case we investigated the Pareto curves for two and respectively three objectives. The two-objectives optimization involved in a first step the determination of the PTV- OAR trade-off curve and in a second instance the PTV-NT Pareto front. For each of the optimization procedure, eleven points per Pareto front were calculated, meaning that there were eleven combinations of importance factors corresponding to the two objectives. The importance factor values were varied in steps of 0.1. For all optimizations, the critical dose values for the OAR and normal tissue were set to 20% and 30% of the dose delivered to the reference point, usually the isocentre.

The trade-off curves for the two optimizations performed with the above parameters are shown in *Figure 4*. Both curves represent the values of the objective values normalized to their largest values, obtained when the corresponding importance factors equal unity.

Each point of the curves is a certain combination of importance factors. Now, having the Pareto curves, the decision-maker can select those solutions which suit better either the PTV objective, or respectively, the OAR objective. For instance, in *Figure 4*, if one would like to see the optimization results consistent with good target homogeneity, then points with smaller PTV objective value should be selected. Generally a good investigation start for the verification of the dose distributions and DVHs involves the Pareto point closest to the “utopia point” defined as the point with the objective value being zero (the origin of the  $f_1$ - $f_2$  coordinate system).

In *Figure 4*, the point labeled *Pt.3* and characterized by  $w_{PTV}=0.8$  and  $w_{OAR}=0.2$  has the closest distance to the origin, which means that its corresponding solution offers good performances against both the PTV dose homogeneity and the OAR protection. The corresponding dose distribution for this particular Pareto point is displayed in *Figure 5A*, where one can see that the PTV is fully covered by the 95% isodose. Though, if the decision maker considers that the critical structure is sufficiently protected, then he could investigate the solution corresponding to *Pt.2* ( $w_{PTV}=0.9$  and  $w_{OAR}=0.1$ ) in order to determine whether what is being lost for the OAR protection constitutes a real gain for the PTV homogeneity improvement. We present in *Figure 6A* the DVHs corresponding to the two plans. As one can see, little degradation of the PTV objective is observed for the two solutions, while the OAR objective greatly degrades for *Pt.2*( $0.9, 0.1$ ) solution as compared with the *Pt.3*( $0.8, 0.2$ ). Conversely, if the decision maker considers the OAR protection objective more restrictive, he then could make the investigation towards the point 4 of the Pareto curve.

The same test case was used in order to determine the trade-off curve for other two objectives, namely the PTV and the normal tissue (NT). The Pareto curve for the PTV-NT objectives is shown with circles in *Figure 4*. It is important to note the different shape and point distribution along the two curves representing the PTV-OAR and PTV-NT trade-off curves. A certain PTV objective value obtained from the PTV-OAR trade-off curve is calculated for a particular combination of importance factors, which differ consistently from the importance factors combination corresponding to the same PTV value of the other PTV-NT Pareto curve.

Similarly as for the PTV-OAR objectives, in the case of the PTV-NT objectives one could select points 9 and 10 for dose distribution and DVHs estimation. The dose distribution corresponding to the point 9 ( $w_{PTV}=0.2$  and  $w_{NT}=0.8$ ) of the corresponding Pareto curve is depicted in *Figure 5B*. It is worth noting here how well the high isodose lines are “attracted” to the PTV contour, as compared to the dose distribution presented in *Figure 5A*.

The optimization performed simultaneously for all the three objectives (PTV, OAR and NT) involved the calculation of beamlet weights for 121 different importance factors combinations, as shown in the flow diagram represented in *Figure 2*. The iterations are grouped in 11 sets where the importance factor for the PTV is varied continuously from 0 to 1 in increments of 0.1. The difference  $1-w_{PTV}$  is allocated to the OAR and NT. Every of the above set has at its turn 11 subsets, where only  $w_{OAR}$  and  $w_{NT}$  are varied in increments of 0.1 but their sum equals unity. Therefore, the possible values of the importance factors for OAR and NT can be expressed as  $(1-w_{PTV})(w_{OAR} + w_{NT})$ . This fact implies that for a complete cycle of the  $w_{PTV}$  values, the ratio  $w_{OAR}/w_{NT}$  is constant.

*Figure 7* contains the plots of the trade-off curves for the PTV-OAR and PTV-NT objectives. Due to the possible values of the  $w_{OAR}/w_{NT}$  ratios, the decision process is not limited just at the analysis of one curve, but the whole set of curves. For reasons of simplicity, in *Figure 7*, we represent only few the Pareto curves corresponding to some importance factors combinations. There is a correspondence between the two sets of

curves, meaning that by selecting a point on a particular  $w_{OAR}/w_{NT}$  PTV-OAR curve one can find its correspondent in the PTV-NT representation, and read the third objective value.

In *Figure 7A*, one can see that there is no much difference between the curves having different ratios  $w_{OAR}/w_{NT}$  except the first two ones, for which  $w_{NT}=0.0$  and  $w_{OAR}/w_{NT} = 0.11$ . As compared with the other curves on the same plot, these ones show large objective values for both PTV and OAR. On the other hand, the other curves show smaller PTV-OAR objective values, but they almost superimposed. Therefore, in the selection process of an appropriate Pareto point there would not make much difference which Pareto curve from the latter ones would be chosen. Though, the difference comes when looking at the plot in *Figure 7B*, where the differences are significant with respect to the NT objective. As mentioned for the two-objectives decision process, a good start would be to select a point located close to the origin of the PTV-OAR plot. Let this point be point 9 on the  $w_{OAR}/w_{NT}=0.25$  curve (open circles). The objective values are:  $Obj_{PTV} = 0.022$ ,  $Obj_{OAR} = 0.029$ ,  $Obj_{NT} = 0.143$ , and the corresponding values of the importance factors are:  $w_{PTV} = 0.2$ ,  $w_{OAR} = 0.16$ ,  $w_{NT} = 0.64$ . The dose distribution and DVHs corresponding to the beamlet weights obtained for this set of importance factors are shown in *Figure 5C* and *Figure 6B*. If one take a closer look to the dose distributions presented in *Figure 5*, one could remark that the dose conformation to the PTV is excellent in all the cases. The differences are consistent with how much the low isodose lines expand within the NT for those cases which do not consider the NT objective (5A and 5B). It is worth noting that the shrinkage of the low isodose lines in *Figure 5C* as compared to 5A does not affect the dose to the OAR, which seems similar in the two figures.

In principle, the decision-making operation for cases involving more objectives can be made somehow automated if one considers the euclidian distance of the Pareto point in the objective space. The automated procedure could start by finding the closest to utopia Pareto points (for every  $w_{OAR}/w_{NT}$  curve) in a two dimensional projection of the Pareto surface on the plane involving the most important objectives. Then, sliding from one Pareto point to the next, located on a higher ratio curve, one could find the rest of the objective values.

The calculation time per Pareto point was 15 seconds of CPU time (in the case where all the 75 iterations were accomplished and the tolerance condition was not met), and the whole optimization lasted for thirty minutes. The optimization was performed on a personal computer equipped with a PENTIUM III 1 GHz processor and 512 MB of RAM.

### 3.2. Prostate case

The prostate case involved the dose optimization for five structures grouped in four objectives. The first objective considers the dose homogeneity within the prostate (PTV), while the second and third objectives quantify the protection to the Bladder (B) and Rectum (R), respectively. The critical dose values for these structures were chosen as percentages from the PTV prescription value: 25% for the rectum and 25% for the bladder. The fourth objective comprised the left and the right femoral heads (LFH and RFH) having both as dose tolerance 45% of the PTV prescription value.

Nine equispaced beams were used for optimization:  $0^\circ$ ,  $40^\circ$ ,  $80^\circ$ ,  $120^\circ$ ,  $160^\circ$ ,  $200^\circ$ ,  $240^\circ$ ,  $280^\circ$  and  $320^\circ$  degrees (respecting the IEC convention). The width of the pencil defined at the isocenter was 0.5 cm.

The optimization was performed for 1331 combinations of importance factors. Since for four and more objectives the Pareto surfaces are difficult to visualize every solution was ranked according its distance to the origin of the objective's coordinate system. For four

objectives, this distance was expressed as  $\sqrt{\sum_{i=1}^4 Obj_i^2}$ . The DVHs for the solution

characterized by the smallest distance to the origin is displayed in *Figure 8*. The values of the corresponding importance factors found for this solution were:  $w_{PTV}=0.2$ ,  $w_{Bladder}=0.24$ ,  $w_{Rectum}=0.112$  and  $w_{Femurs}=0.448$ . The user can select another solution from the pool of existing solutions, since these are indexed according their euclidian distance and values of the importance factors. Therefore, if the user is not satisfied with one of the objective performance, he always can search for another solution characterized by a smaller distance to the origin of objectives space, but with a larger importance factor of the less fulfilled objective.

#### 4.- Conclusions

A multiobjective gradient based algorithm was developed for the purpose of dose distribution optimization in external beam conformal radiotherapy. This algorithm is based on an *a priori* approach, gathering the values of all objectives in a single value. The weighting factors of the composite objective values were varied in different steps, allowing eventually reconstructing at the end of the optimization the trade-off surfaces or curves, which define the boundary between the feasible and non-feasible domain regions. The analysis of these curves allows the decision-maker to select the most appropriate solution according to the clinical goals. This work tries to emphasize the fact that a correct selection of the importance factors to multiply the individual objectives in the global objective value is not trivial, and that the determination of the boundary region between the feasible and non-feasible solution regions is highly desirable. This is proved for the C-shaped tumor case, where for the PTV-OAR and PTV-NT trade-off curves, the importance factors corresponding to the points with good dose distributions have very different values, *eg.* 0.8 and 0.2 respectively (see *Figure 4*). Furthermore, the proposed algorithm delivers at the end of optimization a set of solution and not a single one, as other methods (stochastic or deterministic) do.

The gradient-based algorithm hereby described converges very fast. It usually needs less than 75 iterations to reach a consecutive reduction of the global objective of 0.001% of the current iteration objective value. Due to its high convergence rate it can be used to calculate many points located on the Pareto surface. The study hereby presented involved the optimization of 11, 121 and 1331 Pareto points, when there were two, three and respectively four objectives to be optimized. In our opinion, this constitutes a limitation of the algorithm, because most of the clinical cases could involve more than four structures for which constraints are to be imposed. Furthermore, for more than three objectives, the computation time is significantly large (up to three hours on a Pentium III 1GHz processor for the four objectives optimization).

The mathematical form of the objective functions used in this study allowed the analytic calculation of the first derivative, fact that speeded up the calculation time by an important factor. Any kind of objective function can be used, but care should be taken about its convexity. In these cases, the algorithm is provided with the possibility to calculate numerically the first derivative. Of course, this is in detriment of the speed.

A novelty that the developed gradient-based algorithm brings for these optimization methods in conformal radiotherapy refers the positivity constraints imposed on the optimization variables. All the gradient based optimization algorithms presented in literature up to now set at the end of each iteration the negative optimization variables (beamlet weights) to zero. This was not necessary in our algorithm, since the square roots of the beamlet weights were considered for optimization. As a result, at the end of each iteration, only positive values were encountered. Thus, the optimization process occurs more naturally, and probably reduces the number of iterations necessary to reach the optimum.

The test cases hereby investigated involved the optimization of the beam intensity profiles just for the central slice which contained 4096 sampling points (uniformly distributed on a rectangular grid). Since for a full three-dimensional optimization one could use the same density of sampling points, but quasi-randomly distributed within the volume, the foreseen calculation times would not differ essentially as for the presented cases. At the time being we are in the process of extending the method for the three-dimensional geometry and code optimization. As far as the decision process is concerned, there would be possible to rank the obtained plans based on a DVH score function, but this would further reduce the speed of the algorithm.

The multiobjective optimization method hereby described can be used as a tool for obtaining the best values of importance factors for different clinical test cases. Thus, it may come in competition with other proposed methods, which aim at determining the values of the importance factors for template clinical cases. Another use would be to give a good initial solution for other stochastic algorithms like simulating annealing or genetic algorithms, because these methods do not provide until now the powerful insight into the multiobjective optimization.

## References

- Bortfeld T, Burkelbach J, Boesecke and Schlegel W, 1990, Methods of image reconstruction from projections applied to conformation radiotherapy, *Phys. Med. Biol.* **35** 1423-34.
- Cotrutz C, Kappas C, Theodorakos Y, Makris C and Mohan R, 1998, Development in a Windows environment of a radiation treatment planning system for personal computers, *Comput. Methods Progr. Biomed.* **56** 261-72.
- Deasy J O, 1997, Multiple local minima in radiotherapy optimization problems with dose-volume constraints, *Med. Phys.* **24** 1157-61.
- Deb K., 1999, Evolutionary algorithms for multi-criterion optimization in engineering design. In *Proceedings of Evolutionary Algorithms in Engineering and Computer Science (EUROGEN'99)* 1-30.
- Gustafsson A, Lind B K and Brahme A., 1994, A generalised pencil beam algorithm for optimization of radiation therapy, *Med. Phys.* **21** 343-56.
- Hristov D H and Fallone B G, 1997, An active set algorithm for treatment planning optimization, *Med. Phys.* **24** 1455-64.
- Hristov D H and Fallone B G, 1998, A continuous penalty function method for inverse treatment planning, *Med. Phys.* **25** 208-23.
- Mageras G S and Mohan R, 1993, Application of fast simulated annealing to optimization of conformal radiation treatments, *Med. Phys.* **20** 639-47.
- Mohan R, Mageras G S, Baldwin B, Brewster L J, Kutcher G J, Leibel S, Burman C M, Ling C C and Fuks Z, 1992, Clinically relevant optimization of 3D conformal treatments, *Med. Phys.* **19**, 933-44.
- Press W H, Teukolsky S A, Vetterling W T and Flannery B P, 1992, Numerical Recipes in C, 2<sup>nd</sup> ed. (Cambridge U.P., New York).
- Soderstrom S and Brahme A, 1993, Optimization of the dose delivery in a few field techniques using radiobiological objective functions, *Med Phys.* **20** 1201-9.
- Spirou S V, and Chui C S, 1997, A gradient inverse planning algorithm with dose-volume constraints, *Med. Phys.* **25** 321-33.
- Wang X, Mohan R, Jackson A, Leibel S A, Fuks Z and Ling C C, 1995, Optimization of intensity-modulated 3D conformal treatment plans based on biological indices", *Radiother. Oncol.* **37** 140-152.
- Webb S, 1989, Optimization of conformal radiotherapy dose distributions by simulated annealing, *Phys. Med. Biol.* **34** 1349-69.
- Wu Q and Mohan R, 2000, Algorithms and functionality of an intensity modulated radiotherapy optimization system, *Med. Phys.* **27** 701-11.
- Wu X and Zhu Y, An optimization method for importance factors and beam weights based genetic algorithms for radiotherapy treatment planning, *Phys. Med. Biol.* **46** 1085-99.
- Xing L, Li J G, Donaldson S, Le Q T and Boyer A L, 1999, Optimization of importance factors in inverse planning, *Phys Med. Biol.* **44** 2525-36.

Yu Y, 1997, Multiobjective decision theory for computational optimization in radiation therapy, *Med. Phys.* **24(9)** 1445-54.

## Figure Captions

- Figure 1:** Illustration of a convex solution set  $\mathbf{F}$  for the case of two objectives ( $f_1$  and  $f_2$ ) minimization. The AB side of the convex set is formed out of solutions (like points 1 and 2) which are not dominated by any other solutions (like point 4) of the set  $\mathbf{F}$ .
- Figure 2:** Flow diagram of the optimization process. The current scheme is exemplified for  $j+1$  objectives optimization, whose importance factors noted with  $w_{PTV}$  and  $w_{OAR1} \dots w_{OARj}$ .
- Figure 3:** Convergence rate of the investigated Polak-Ribiere conjugate gradient algorithm. The convergence rate was investigated for two objectives: the C-shaped PTV and the circular OAR and three combinations of importance factors.
- Figure 4:** Pareto fronts for the C-shaped tumor case: the squares represent the Pareto points for the PTV-OAR objectives and the circles are the Pareto points for the PTV-Normal Tissue objectives. Every objective value is normalized to its maximum, obtained when the corresponding importance factor is set to unity.
- Figure 5:** Dose distributions for the C-shaped tumor case: **A:** PTV-OAR objectives ( $w_{PTV}=0.8$ ,  $w_{OAR}=0.2$ ); **B:** PTV-NT objectives ( $w_{PTV}=0.8$ ,  $w_{OAR}=0.2$ ); **C:** PTV-OAR-NT objectives ( $w_{PTV}=0.2$ ,  $w_{NT}=0.8$ );
- Figure 6:** Dose Volume Histograms for PTV, circular OAR and Normal Tissue (NT) for the C-shaped tumor case. **A:** PTV and OAR DVHs corresponding to plan obtained for points 2 ( $w_{PTV} = 0.9$ ;  $w_{OAR}=0.1$ ) and 3 ( $w_{PTV} = 0.8$ ;  $w_{OAR} = 0.2$ ) of the PTV-OAR Pareto front. **B:** PTV, OAR and NT DVHs corresponding to plan obtained for point 9 (*Figure 7*).of the  $w_{OAR}/w_{NT} = 0.25$  Pareto curve of the three dimensional optimization. The corresponding importance factors are:  $w_{PTV} = 0.2$ ,  $w_{OAR}=0.16$  and  $w_{NT} = 0.64$ .
- Figure 7:** Pareto trade-off curves for the PTV-OAR objectives (**A**) and PTV-NT objectives (**B**) for the C-shaped tumor three objectives optimization.
- Figure 8:** DVHs for the prostate case obtained for the following combination of the importance factors:  $w_{PTV} = 0.2$ ,  $w_{Bladder} = 0.24$ ,  $w_{Rectum} = 0.112$  and  $w_{Femurs} = 0.448$ . The following structures were involved in the optimization: Planning Target Volume (PTV), Bladder (B), Rectum (R), Left Femoral Head (LFH) and Right Femoral Head (RFH).

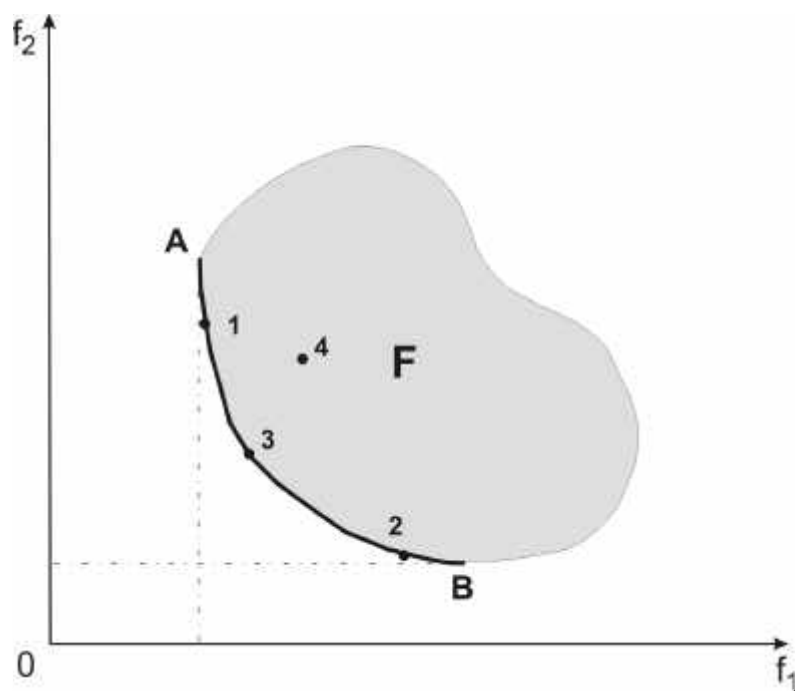


Figure 1

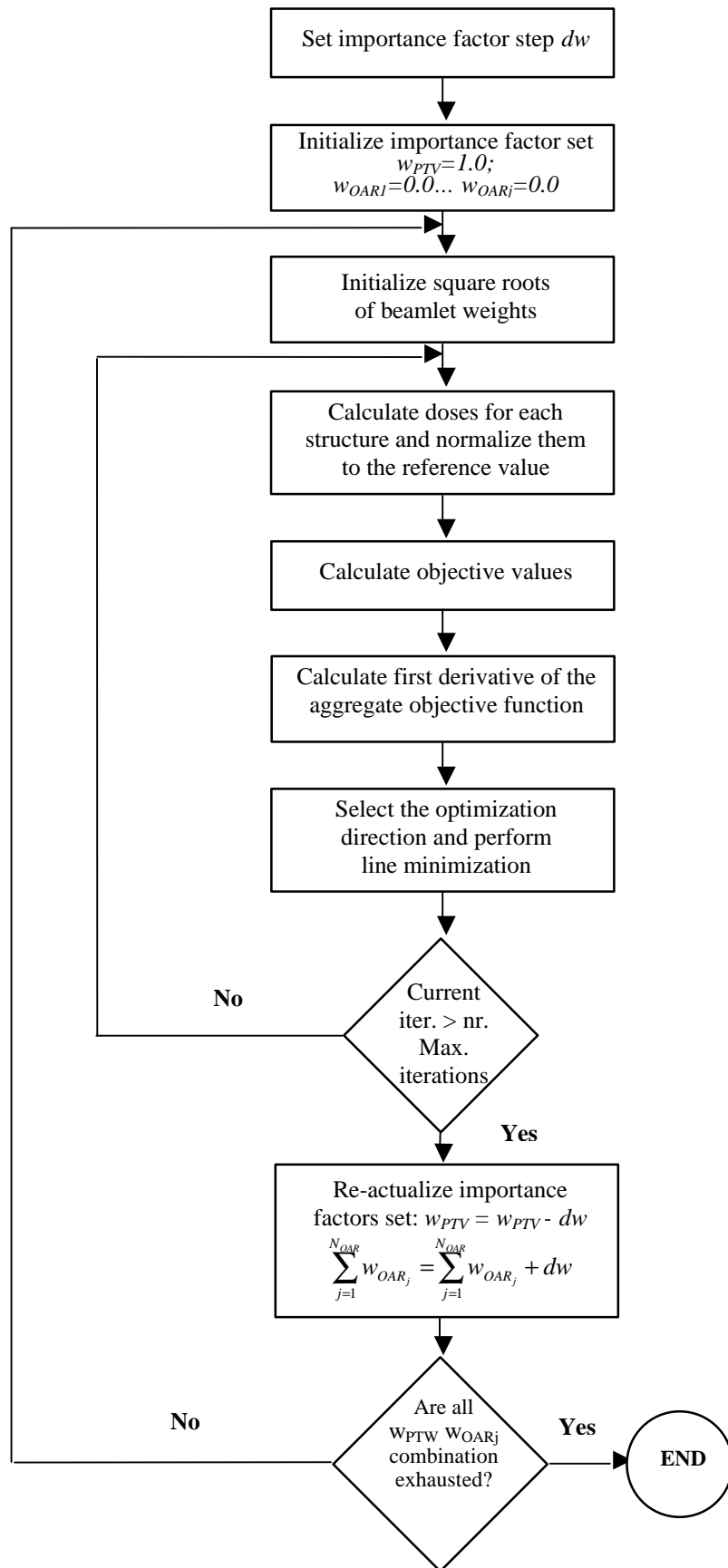


Figure 2

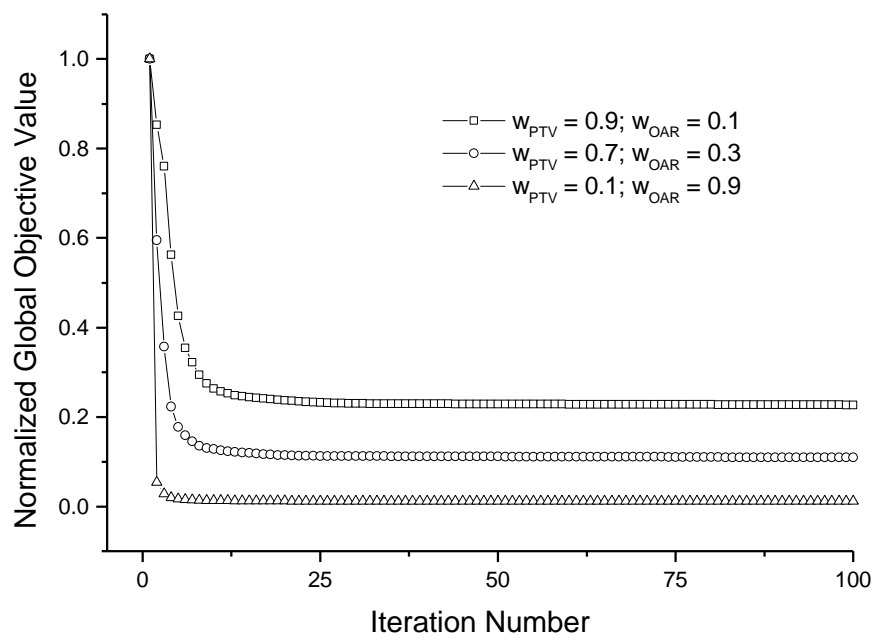


Figure 3

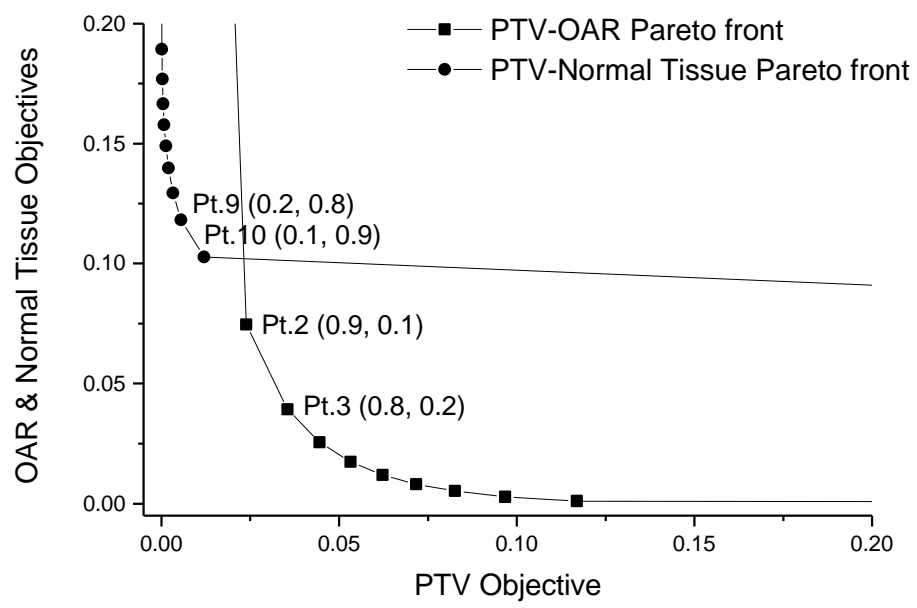


Figure 4

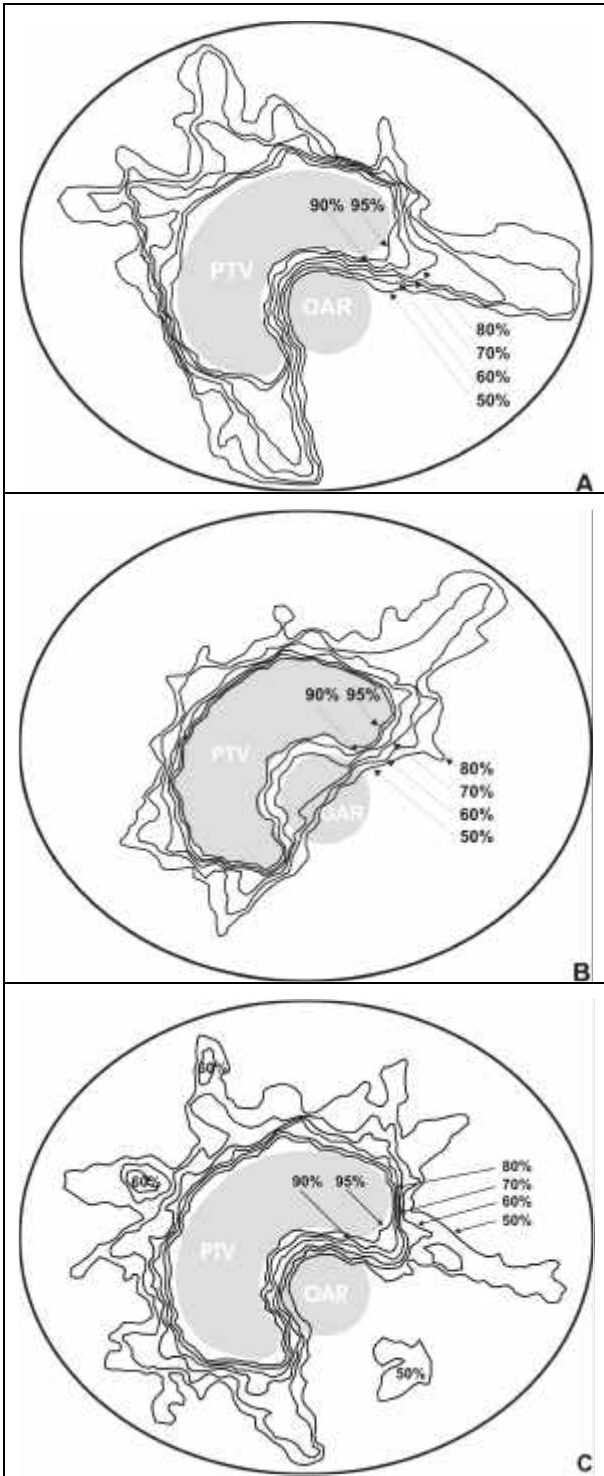


Figure 5

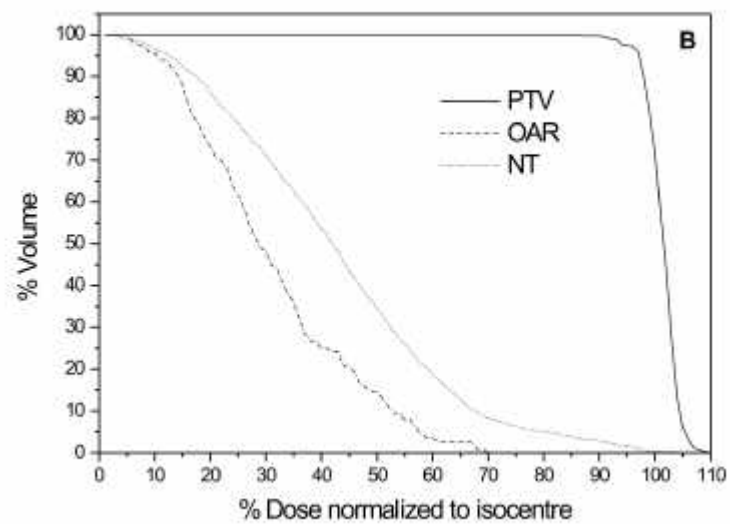
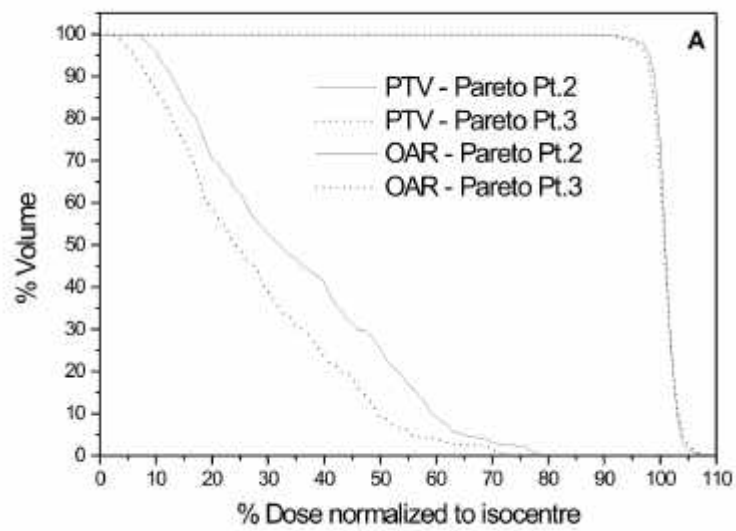


Figure 6

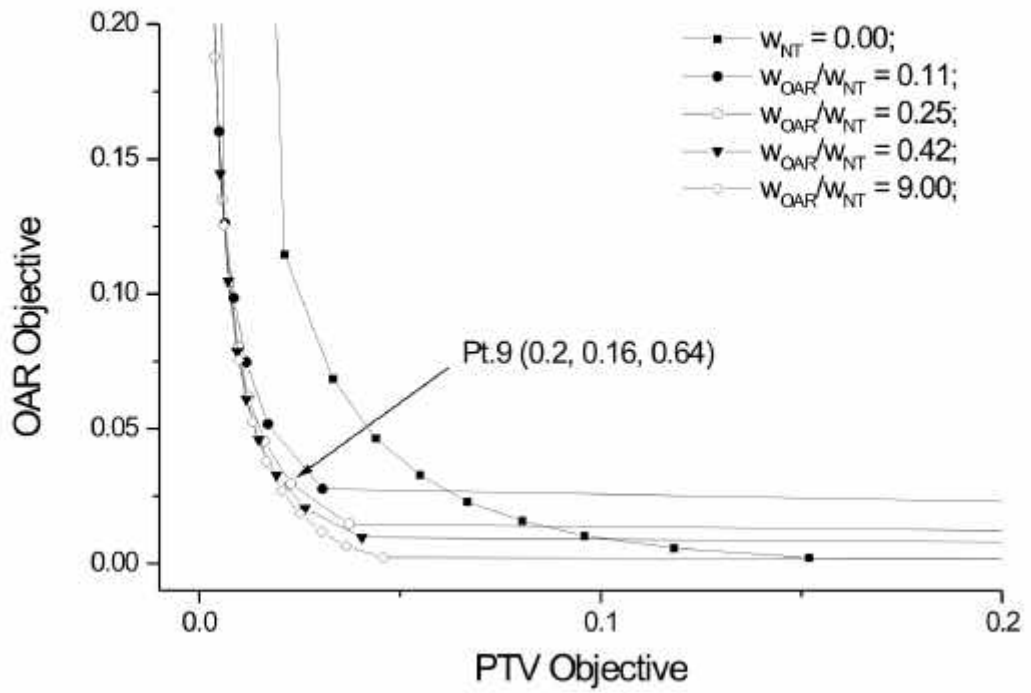
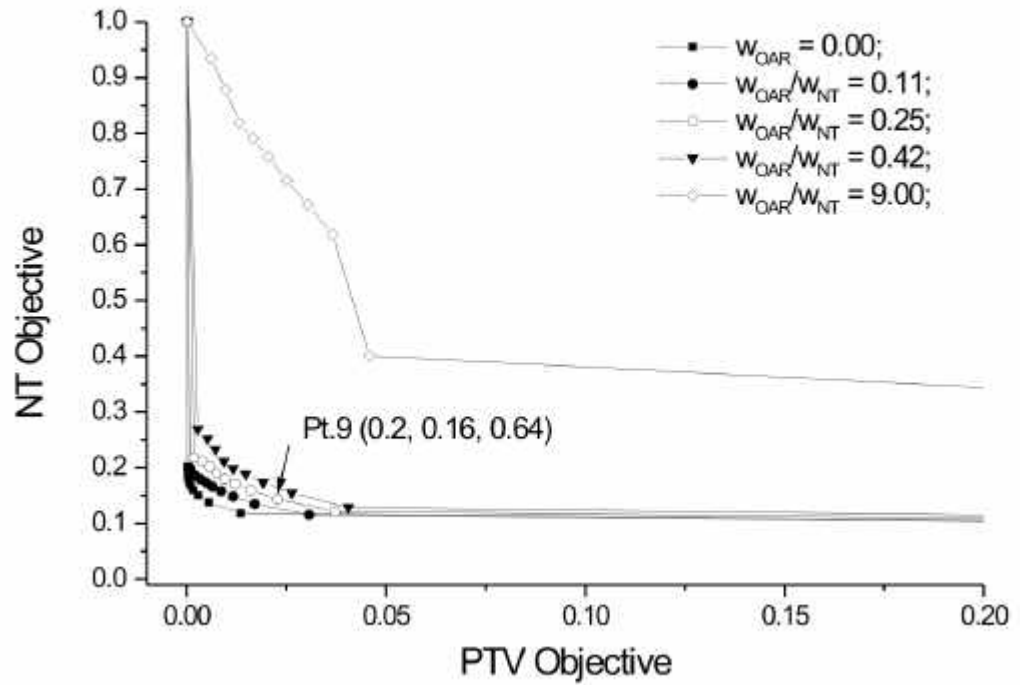
**A****B**

Figure 7

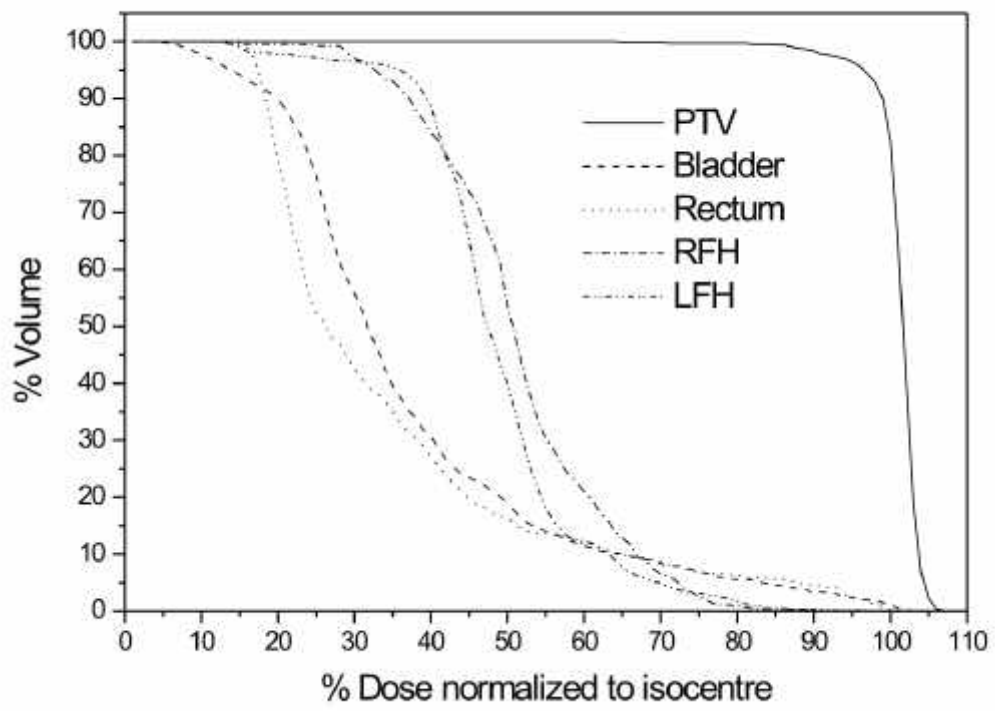


Figure 8